Food Hydrocolloids 162 (2025) 110933

Contents lists available at ScienceDirect

Food Hydrocolloids

journal homepage: www.elsevier.com/locate/foodhyd

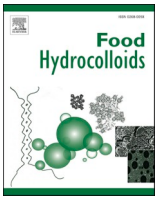

Plasticized cellulose bioplastics with beeswax for the fabrication of multifunctional, biodegradable active food packaging

Pedro Florido-Moreno [a], José J. Benítez [b], Jaime González-Buesa [c], José M. Porras-Vázquez [d], Jesús Hierrezuelo [e], Montserrat Grifé-Ruiz [e], Diego Romero [e], Athanassia Athanassiou [f], José A. Heredia-Guerrero [a,**], Susana Guzmán-Puyol [a,*]

[a] Instituto de Hortofruticultura Subtropical y Mediterránea "La Mayora", Universidad de Málaga-Consejo Superior de Investigaciones Científicas (IHSM, UMA-CSIC), Bulevar Louis Pasteur 49, 29010, Malaga, Spain
[b] Instituto de Ciencia de Materiales de Sevilla, Centro Mixto CSIC-Universidad de Sevilla, Calle Américo Vespucio 49, Isla de la Cartuja, 41092, Seville, Spain
[c] Departamento de Ciencia Vegetal, Centro de Investigación y Tecnología Agroalimentaria de Aragón (CITA), Instituto Agroalimentario de Aragón - IA2 (CITA-Universidad de Zaragoza), Av. Montañana 930, 50059, Zaragoza, Spain
[d] Departamento de Química Inorgánica, Cristalografía y Mineralogía, Universidad de Málaga, 29071, Malaga, Spain
[e] Instituto de Hortofruticultura Subtropical y Mediterránea "La Mayora", Universidad de Málaga-Consejo Superior de Investigaciones Científicas (IHSM, UMA-CSIC), Departamento de Microbiología, Bulevar Louis Pasteur 49, 29010, Malaga, Spain
[f] Smart Materials Group, Istituto Italiano di Tecnologia, Via Morego 30, 16163, Genova, Italy

ARTICLE INFO

Keywords:
Food packaging
Cellulose
Beeswax
Bioplastics
Barrier properties

ABSTRACT

Plasticized cellulose bioplastics with antioxidant and antimicrobial properties were prepared by blending cellulose and glycerol in a mixture of trifluoroacetic acid and trifluoroacetic anhydride, adding a solution of beeswax in chloroform, and subsequent drop-casting. Optical, chemical, structural, mechanical, thermal, and hydrodynamic properties were fully characterized. In addition, the biodegradability in seawater was investigated by determination of the biological oxygen demand. The incorporation of beeswax ruled out the transparency and UV blocking, modified the main mechanical parameters, and improved the thermal stability and the antioxidant capacity, as well as the hydrodynamic and barrier properties. In general, these features were comparable to those of common petroleum-based food packaging plastics. Such changes were explained by the incorporation of beeswax into the polymer matrix, as determined by infrared spectroscopy and X-ray diffraction. These cellulose-beeswax bioplastics were evaluated as viable food packaging materials by determination of the overall migration by using Tenax® as a dry food simulant, oxygen permeability at different relative humidities, measurement of antimicrobial activity against *Escherichia coli* and *Bacillus cereus*, and through preservation of fresh-cut pear slices, showing results similar to those obtained by using low-density polyethylene.

1. Introduction

The rapid growth of the world population, which has exceeded 8 billion and is expected to reach over 9.7 billion by 2050, has increased the demand for efficient food packaging solutions (Smith, 2015). Food packaging plays an important role in preserving the nutritional quality and freshness of food products during transport and storage, especially in densely populated and urban areas where supply chains are complex and lengthy (Aubry & Kebir, 2013). Conventional petroleum-based plastics have long dominated the food packaging industry due to their easy processability, durability, cost-effectiveness, and excellent barrier properties, among others (Marsh & Bugusu, 2007). However, these materials contribute to environmental degradation, resource depletion, and persistent plastic pollution. For this reason, their substitution has become a target for researchers, policymakers, and citizens (Geyer, Jambeck, & Law, 2017). Among the different solutions, natural biopolymers such as polysaccharides, polyesters, and proteins, to mention a few, present a promising alternative due to their inherent biodegradability and reduction of the carbon footprint (Siracusa, Rocculi, Romani, & Rosa, 2008). In particular, polysaccharide-based bioplastics are

* Corresponding author.
** Corresponding author.
E-mail addresses: ja.heredia@csic.es (J.A. Heredia-Guerrero), susana.guzman@csic.es (S. Guzmán-Puyol).

https://doi.org/10.1016/j.foodhyd.2024.110933
Received 20 September 2024; Received in revised form 15 November 2024; Accepted 2 December 2024
Available online 3 December 2024
0268-005X/© 2024 The Authors. Published by Elsevier Ltd. This is an open access article under the CC BY-NC-ND license (http://creativecommons.org/licenses/by-nc-nd/4.0/).

widely used due to their excellent film forming properties, good oxygen permeability, and the possibility of functionalization through the addition of antimicrobial and antioxidant molecules (Cazón, Velazquez, Ramírez, & Vázquez, 2017). For food packaging uses, cellulose stands out among other polysaccharides due to its low cost, abundant availability, ease of storage and handling, potential for incorporating consumer information and branding, environmental safety, and recyclability (Guzman-Puyol, 2024). In any case, polysaccharide-based materials are usually brittle, water sensitive, and show water permeability values much higher than the accepted values for most of the ready to eat food, limiting their use at commercial scale (Wu, Misra, & Mohanty, 2021). A common strategy to improve the mechanical properties of polysaccharide-based materials is the use of plasticizers (Dong et al., 2023). Plasticizers are low molecular weight substances added intentionally to a polymer material to increase its flexibility (Alee et al., 2021). Consequently, with no plasticizer, polysaccharide-based bioplastics are mechanically brittle due to the strong interaction between polymer chains. When a plasticizer is used, the interaction between polymer chains is reduced and the flexibility of the material and its resistance to fracture are increased (Vieira, da Silva, dos Santos, & Beppu, 2011). The most common plasticizers for polysaccharides are hydrophilic molecules such as glycerol, polyethylene glycol, and sorbitol (Andreuccetti, Carvalho, & Grosso, 2009). In the case of pure cellulose bioplastics, the addition of glycerol has recently been proposed to plasticize the cellulose matrix. This results in a ductilization of the mechanical parameters (Benitez et al., 2024). However, a side effect of using hydrophilic plasticizers in combination with polysaccharide matrices is a worsening of the water uptake and barrier properties as a result of a higher number of hydroxyl groups able to interact with water in both liquid and vapor states (Trinh, Chang, & Mekonnen, 2023).

In order to improve their hydrodynamic properties, different strategies have been proposed. For example, fluorinated compounds have been used for decades due to their excellent hydrophobic and oleophobic properties, although some of these compounds, usually known as perfluoroalkyl compounds (PFAS) are highly persistent in the environment (Pascale et al., 2023). Other alternatives to these "forever chemicals" are natural hydrophobic molecules such as lipids, fatty acids, waxes, and resins. Waxes are a family of nonpolar substances and are considered very efficient molecules to reduce moisture permeability (Morillon, Debeaufort, Blond, Capelle, & Voilley, 2002). Main commercially available waxes include beeswax, carnauba wax, and candelilla wax. Beeswax, a type of a natural waxes produced by honeybees of the genus *Apis*, consists of a complex mixture of hydrocarbons, fatty acids, esters, and fatty alcohols (Peron et al., 2023). Beeswax has been largely described for its antimicrobial and anti-inflammatory activities, wound healing, dermatological, cosmetic, and antioxidant properties (Cornara, Biagi, Xiao, & Burlando, 2017). In the food industry, beeswax is a food additive (E−901) approved by the European Union and used as glazing agent, coating, and carrier for flavor (EFSA, 2007). In general, this type of hydrophobic molecules, both fluorinated and waxes compounds, are typically incorporated in cellulose systems by coating, lamination, and internal and external sizing (Guzman-Puyol, 2024).

This work proposes the fabrication of transparent, biodegradable, and high-barrier bioplastics from glycerol-plasticized cellulose and beeswax by using trifluoroacetic acid (TFA) and trifluoroacetic anhydride (TFAA) as a solvent mixture, as previously reported for other crystalline materials such as chitin (Heredia-Guerrero et al., 2023), plant wastes (Bayer et al., 2014), and cellulose derivatives (Guzman-Puyol, Tedeschi, et al., 2022; Tedeschi et al., 2021). In this case, we have used a glycerol content of 30% due to, at this proportion, the blend shows ductile properties similar to other common commodity plastics (Benitez et al., 2024). Here, the effect of the beeswax addition on the optical, chemical, structural, thermal, antioxidant, barrier properties, and biodegradability was systematically studied and compared with other food packaging materials. The beeswax percentages used in this work were between 0 and 20% in order to have a wide range of concentrations that allow to understand correctly the role of the waxes in the final properties of the blends. Finally, the potential of these materials for food packaging has been demonstrated by preservation of pear slices as a real food.

2. Experimental part

2.1. Materials

Microcrystalline cellulose, glycerol, beeswax, trifluoroacetic acid (TFA), trifluoroacetic anhydride (TFAA), lithium chloride (LiCl), sodium bromide (NaBr), potassium chloride (KCl), 2,2-diphenyl-1-picrylhydrazyl radical (DPPH·), and Tenax® (a porous poly(2,6-diphenyl-*p*-phenylene oxide) material) were acquired from Sigma-Aldrich. Toluene, heptane, chloroform, and castor oil were supplied by VWR. All solvents and reagents were used as received. Low density polyethylene (LDPE) film and commercial mature "Conference" pears were acquired in a local market (Malaga, Spain).

2.2. Fabrication of plasticized cellulose-beeswax bioplastics

Plasticized cellulose films were prepared by dissolving different amounts of cellulose (315–252 mg) at 50 °C for 45 min in a 50 mL closed flask containing 30 mL of a TFA:TFAA mixture (2:1, v:v). Then, 30 wt% glycerol was added and vigorously mixed. This glycerol content was chosen due to the improvement of mechanical properties of cellulose for food packaging applications, as previously reported (Benitez et al., 2024). Finally, beeswax solutions (1 wt%) in chloroform were added to the cellulose-glycerol solutions according to the formulations of Table 1. Solutions were casted on glass Petri dishes and left to dry overnight. ~70 μm free-standing films were obtained. All films were conditioned at a temperature of ~23 °C and a relative humidity of ~44% before testing. Samples were designated as CGW-x where "C" is for cellulose, "G" is for glycerol, "W" is for beeswax, and "x" indicates the weight percentage of beeswax.

2.3. Optical characterization

A VWR 6300 UV–Vis (VWR International, Belgium) was used to obtain the transmittance spectra in the range 200–800 nm. T_{600nm} was used to quantify the transparency. Ultraviolet radiation blocking was calculated in the UV-A (315–400 nm), UV-B (280–315 nm), and UV-C (200–280 nm) regions as follows:

$$UV-x\ blocking\ (\%) = 100 - T_{UV-x} \quad (1)$$

where $T_{UV\text{-}x}$ is the average transmittance in the corresponding UV region. Three measurements were performed per each sample and the results were averaged.

2.4. Morphological characterization

The surface morphology of CGW bioplastics was examined by coating the samples with a ~10 nm layer of gold using a JEOL ION SPUTTER JFC 1100. After, top-view scanning electron microscopy (SEM) images were acquired with a JEOL JSM-6490LA microscope under high vacuum and an acceleration voltage of 15 kV.

2.5. Chemical and structural characterization

Fourier-transform infrared (FTIR) spectra were obtained using a Nicolet IS50 spectrometer (Thermo Scientific) equipped with a single-reflection attenuated total reflection (ATR) accessory (Smart Performer, Thermo Nicolet) in the range 4000–650 cm^{-1}, accumulating 128 scans, and a spectral resolution of 4 cm^{-1}. Measurements were taken

Table 1
Labeling and formulation of CGW samples.

Label	$m_{cellulose}$ (mg)	$m_{glycerol}$ (mg)	$m_{beeswax}$ (mg)	Cellulose (wt%)	Glycerol (wt%)	Beeswax (wt%)
CGW-0	315.0	135.0	0.0	70.0	30.0	0.0
CGW-1	311.9	133.7	4.5	69.3	29.7	1.0
CGW-2.5	307.1	131.6	11.3	68.3	29.2	2.5
CGW-5	299.3	128.3	22.5	66.5	28.5	5.0
CGW-10	283.5	121.5	45.0	63.0	27.0	10.0
CGW-15	267.8	114.8	67.5	59.5	25.5	15.0
CGW-20	252.0	108.0	90.0	56.0	24.0	20.0

in three distinct regions within each sample.

Structural characterization was performed by X-ray diffraction (XRD) on a Rigaku SmartLab X-ray diffractometer with a copper rotating anode X-ray source operating at 40 kV and 150 mA and a Gobel mirror to produce a parallel beam and minimize Cu Kβ radiation. Measurements were conducted using a 2θ scanning method and XRD intensity values were normalized to the maximum intensity. The crystallinity index was determined using the following equation:

$$Crystallinity\ index = \frac{I - I'}{I}\ x\ 100 \quad (2)$$

where I is the intensity of the (002) cellulose crystal plane peak and I′ is the intensity of the amorphous contribution. Moreover, the crystallite size (D) was estimated by using the Scherrer's equation:

$$D = \frac{K\lambda}{\beta \cos\theta} \quad (3)$$

where K is a constant value of 0.94, λ is the X-ray wavelength, β is the peak width at the middle of the maximum intensity, and θ is the diffraction angle for the (200) plane.

2.6. Mechanical characterization

Uniaxial tensile tests were conducted using a MTS Criterion 42 with a 50 N load cell. From stress-strain curves, main mechanical parameters (i.e., Young's modulus, ultimate tensile strength, strain at break, and toughness) were calculated. Five to ten replicates were measured per each sample and the mechanical parameters were averaged and the corresponding standard deviation calculated.

2.7. Thermal characterization

Thermal stability of CGW films was assessed by thermogravimetric analysis with an SDT Q600 (TA instruments). ~3 mg of the different samples were loaded into a platinum pan. Thermograms were obtained from 30 to 600 °C using a heating rate of 5 °C/min and a continuous flow of nitrogen (50 mL/min). From TGA curves, heat resistant index (T_s) was calculated as follows:

$$T_s = 0.49\ (T_{d5} + 0.6\ (T_{d30} - T_{d5})) \quad (4)$$

where T_{d5} and T_{d30} are the temperatures corresponding with the 5% and 30% of weight loss, respectively. TGA was carried out in triplicate for each sample, the heat resistant index values averaged and the corresponding standard deviation calculated.

2.8. Water uptake

Water uptake was assessed by drying the CGW samples in a desiccator until their weight was stabilized. Then, ~80 mg of dried samples were weighed in an analytical balance and placed into chambers with different constant relative humidities (0, 11, 57, 84, and 100% RH) at 25 °C. After 24 h, samples were reweighed and the water uptake was calculated as follows:

$$Water\ uptake\ (\%) = \frac{m_f - m_0}{m_0}\ x\ 100 \quad (5)$$

where m_f and m_0 are the weights after each RH (%) and the sample weight at 0% RH, respectively. Three replicates for each formulation were measured, values averaged and the corresponding standard deviation calculated.

2.9. Wettability, oil resistance, and barrier properties

Surface wettability was assessed by static water contact angle values (WCAs) by using a KSV Attension TL100 goniometer with a CCD camera. The image processing software OneAttension (Biolin Scientific) was used. All measurements were made at room conditions. 2 μL droplets of MilliQ water were used. Up to 10 measurements were carried out randomly for each sample. Results were expressed as average values ± standard deviations.

Grease resistance was performed by following the Tappi test method commonly known as the kit test. This is an assay in which different combinations of castor oil, toluene, and heptane (labeled from 1 to 12) are applied to the top of the samples for 15 s and the surface is checked after that. A dark spot indicates the oil penetration and the test failure. The highest number solution no leaving a dark spot on the sample is chosen as kit test number. Three replicates for each formulation were measured, values averaged and the corresponding standard deviation calculated.

Water vapor transmission rate (WVTR) and water vapor permeability (WVP) were determined following the ASTM E96 standard method. A 100% relative humidity gradient (ΔRH%) was generated at room temperature by using 6 mL of deionized water in the internal part of custom-made aluminum 5.3 cm^2 permeation cells. Then, circular CGW samples were attached to the top of the cells and placed in a desiccator at 0% RH. The weight loss of the permeation cells was hourly measured using an electronic balance and plotted as a function of time to obtain the slope. The WVTR and WVP were calculated as follows:

$$WVTR\ \left(g \bullet m^{-2} \bullet day^{-1}\right) = \frac{Slope}{Area\ of\ the\ film} \quad (6)$$

$$WVP\ \left(g \bullet m^{-1} \bullet day^{-1} \bullet Pa^{-1}\right) = \frac{WVTR \bullet l \bullet 100}{P_s \bullet \Delta RH} \quad (7)$$

where l (m) is the thickness of the sample, ΔRH (%) is the percentage relative humidity gradient, and P_s (Pa) is the saturation water vapor pressure at 25 °C. Measurements were made in triplicate and the results were averaged and the corresponding standard deviation calculated.

Oxygen transmission rates (OTR) were assessed for the CGW samples and for some commercial films such as polylactid acid (PLA) (Earthfirst BCFB, Sidaplax, Ghent, Belgium) and oriented polypropylene (OPP) (Envaflex, Utebo, Spain). OTR was determined at 23 °C and different relative humidities (0, 30, 60, and 90% RH) according to the standard ASTM D3985 method using an OX-TRAN®Model 2/21 (MOCON, USA). The oxygen permeability (OP) of the films was calculated as follows:

$$OP\ \left(kg \cdot m \cdot m^{-2} \cdot s^{-1} \cdot Pa^{-1}\right) = \frac{OTR \cdot l}{\Delta P} \quad (8)$$

where l is the film thickness determined in 5 different spots for each sample and ΔP is the partial oxygen pressure difference across the film. The permeability of two samples from each conditioning treatment, each taken from a different replicate, was measured, values averaged and the corresponding standard deviation calculated.

2.10. Biodegradation in seawater

Biodegradability was assessed by tracking the biological oxygen demand (BOD). To do this, ~200 mg of each sample was finely minced and placed in bottles containing 164 mL of seawater collected from the Malaga shoreline (Spain). Oxygen consumption was monitored at 20 °C during 30 days using OxyTop®-i heads (WTW, Germany). As a negative control, bottles filled with seawater were used. Measurements were made in triplicate.

After BOD assay, the solid remaining in the bottles was filtered, washed with distilled water, and dried for 24 h. Then, the surface morphology was analyzed by SEM and the weight loss was calculated by using the following equation:

$$Weight\ loss\ (\%) = \frac{m_0 - m_f}{m_o} x\ 100 \quad (9)$$

where m_0 and m_f are the sample weights before and after the experiment, respectively. Values averaged and the corresponding standard deviation calculated.

2.11. Antioxidant capacity

The antioxidant capacity of CGW bioplastics was evaluated using the standard DPPH· method. Samples with a diameter of 5 mm were placed into vials containing 3 mL of a 0.1 mM DPPH solution in ethanol and placed in the dark until measurement. A VWR 6300 spectrophotometer was used to register the reduction in the absorbance at 515 nm at various time intervals from 0 to 103 h. The radical scavenging activity (RSA) was then determined as the percentage inhibition of free radicals by the sample, calculated using the following equation:

$$RSA\ (\%) = \frac{A_0 - A_t}{A_0}\ x\ 100 \quad (10)$$

where A_0 and A_t are the initial absorbance and the absorbance at different times, respectively. RSA values were normalized to the weight of the sample. Measurements were made in triplicate, values averaged and the corresponding standard deviation calculated.

2.12. Overall migration

Migration of components from CGW films into food was evaluated by using Tenax® as simulant for dry food according to the plastic FCM Regulation (EU) No October 2011 (European Commission, 2011). For this, samples with a diameter of 20 mm were placed in glass vials with 40 mg of Tenax on the bottom. Then, another 40 mg were placed on the top of the samples. Vials were sealed and stored at (40 ± 0.5)°C for 10 days. After that, circles were reweighted and the overall migration was calculated using the following equation:

$$M = \frac{m_0 - m_f}{S} \quad (11)$$

where M is the overall migration (mg dm^{-2}), m_0 and m_f are the initial and mass of Tenax®, respectively, and S is the sample surface in dm^2. For each sample, three measurements were made and the final migration value was reported as the average ± SD.

2.13. Packaging, storage and quality measurement of fresh-cut pears

Mature pears were first cleaned and cut into slices of ~10 g and directly placed in 50 mL Falcon tubes with 1.5 cm dimeter perforated lids. Holes were covered with selected CGW-0 and CGW-5 bioplastics and low-density polyethylene (LDPE) film fixed with double-sided adhesive tape. Uncovered holes were used as a control. All tubes were kept at (4 ± 1)°C in the fridge at different storage times (0, 2, 4, 7, 11, and 14 days). Weight loss was then calculated as the difference between the initial and the final mass and expressed in percentage.

The area loss of the pear slices was quantified. Photographs of the same pear slices were taken at different time intervals. The background was removed, and the area of each slice was measured in pixels using Corel PHOTO-PAINT 2023 software. The area loss for each sample was calculated using the following formula:

$$Area\ loss\ (\%) = \left(\frac{A_0 - A_t}{A_0}\right) \times 100 \quad (12)$$

where A_0 is the area at day 0 and A_t is the area at days 2, 4, 7, 9, 11, and 14.

Evaluation of browning index was made by using the following equations:

$$Browning\ index\ (BI) = \frac{[100(w - 0.31)]}{0.17} \quad (13)$$

$$w = \frac{(a + 1.75L)}{(5.645L + a - 3.012b)} \quad (14)$$

where L, a and b are the CIELAB color parameters obtained by measuring the fresh-cut pear surface with a CR-10 PLUS (Konica Minolta, Ramsey, USA) color reader. Before measuring, a calibration was made with a standard white plate ($L = 97.94$, $a = 0.22$, $b = 1.33$).

Finally, the antioxidant capacity of the pear slices was evaluated by using the DPPH· assay (Almeida et al., 2011). Briefly, pear slices were homogenized and centrifuged (15000 rpm, 4 °C). The supernatant was then recovered and filtered. After, 30 μL of the pear extract was mixed with 3 mL DPPH radical solution and kept in the dark. The decrease in the absorbance was monitored after 5 h.

All tests described in this section were performed in triplicate and the values averaged and presented with their corresponding standard deviation.

2.14. Antibacterial activity

For the antibacterial assays, *Escherichia coli* (BL21 DH5α, gram-negative) and *Bacillus cereus* (AH 187, gram-positive) were utilized. *E. coli* was cultured in Luria-Bertani (LB) medium (1% tryptone, 0.5% yeast extract, 0.5% NaCl), while *B. cereus* was grown in tryptone yeast (TY) medium (1% tryptone, 0.5% yeast extract, 0.5% NaCl, 10 mM $MgSO_4$, 1 mM $MnSO_4$). Both media were solidified using bacteriological agar at a final concentration of 1.5%.

The antibacterial activity of CGW samples was assessed by incubating single colonies of *E. coli* and *B. cereus*, previously cultured at 37 °C for 3 h. A 100 μL aliquot of bacterial suspension was spread onto LB agar plates, followed by the placement of sterilized 1 cm^2 CGW samples onto the agar surface. Plates were then incubated at 37 °C, and bacterial inhibition was evaluated by visual evaluation for the presence of a clear zone (halo) around the samples, indicative of bacterial growth inhibition.

Retentivity assays were performed by spreading a $1{:}10^4$ diluted overnight bacterial culture onto LB agar plates. UV-sterilized CGW pieces were added and incubated at 37 °C overnight. The CGW samples and the agar beneath them were subsequently incubated in liquid medium for 2 h. Agar without CGW served as the control. Bacterial retention was quantified through spectrophotometric measurements at 600 nm (OD600). All experiments were conducted in triplicate.

3. Results and discussion

3.1. Optical and structural characterization

The morphology of CGW bioplastics was analyzed by SEM, Fig. 1A top. CGW-0 showed a continuous, flat surface. For CGW-5 and CGW-20, non-agglomerated beeswax plates homogeneously distributed were observed, as similarly described in literature for other beeswax-containing composites (Lim, Kim, Ko, & Park, 2015). Fig. 1A bottom shows the photos of CGW-0, CGW-5, and CGW-20 bioplastics on a colored logo. CGW-0 showed the highest transparency due to its amorphous structure after solvent evaporation (Caligiuri et al., 2020; Guzman-Puyol, Hierrezuelo, et al., 2022). Addition of beeswax made the films less transparent, being remarkable the whitish appearance for CGW-5 and, in particular, CGW-20. Transmittance in the UV–Vis range was used to characterize the optical properties of CGW bioplastics, Fig. 1B. In general, the addition of beeswax reduced the transmittance values both in the visible and UV range due to the visible light scattering and UV absorption of beeswax crystals (Liu et al., 2022). Transmittance values at 600 nm (T_{600}) were chosen to determine the transparency, Fig. 1C. A gradually decrease of T_{600} was observed by increasing the beeswax content. For beeswax percentages up to 10 wt%, CGW bioplastics showed transmittance values higher than 80%, typical of the so-called transparent food packaging materials such as low density polyethylene (LDPE), polypropylene (PP), polyvinyl chloride (PVC), and polyvinyl alcohol (PVA) (Guzman-Puyol, Benítez, & Heredia-Guerrero, 2022) and other polysaccharide-based films such as cellulose acetate, hydroxypropyl cellulose, chitin, and chitosan (Heredia-Guerrero et al.,

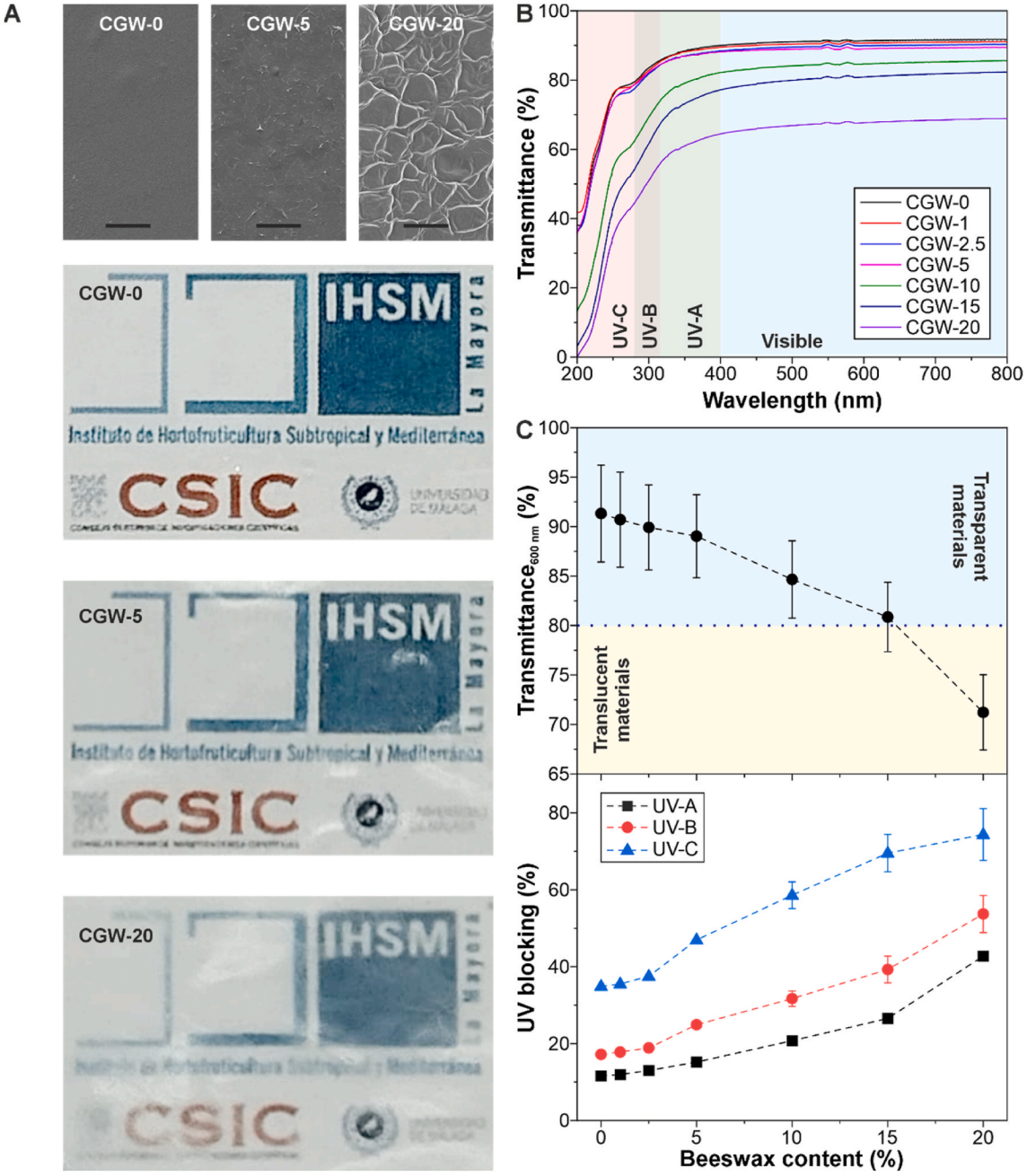

Fig. 1. **A**, top, SEM images (scale bar: 10 μm) and, bottom, photographs on a colored image of CGW-0, CGW-5, and CGW-20. **B**, transmittance of CGW samples in the UV–visible range. The visible, UV-A, UV-B, and UV-C regions and highlighted in different colors. **C,** transmittance values at 600 nm and UV blocking as a function of beeswax content.

2023). For the highest beeswax content, CGW-20 bioplastic showed a transmittance value of ~71%, falling into the category of translucent materials such as semicrystalline polylactide (PLA) (Guzman-Puyol, Benítez, & Heredia-Guerrero, 2022). From transmittance spectra, the UV blocking was calculated, Fig. 1C. CGW-0 showed the lowest UV blocking, with values of ~11.6, ~17.2, and ~34.9% in the UV-A, UV-B, and UV-C, respectively. The incorporation of beeswax improved the UV blocking values, as previously described for other waxes (Baghi, Gharsallaoui, Dumas, & Ghnimi, 2022; Ezati et al., 2023), with values, for instance, of ~17.2, ~24, and ~47.2% in the UV-A, UV-B, and UV-C regions for CGW-5 and ~48.4, ~59.4, and ~83.7% in the respective UV regions for CGW-20. Such an increase in UV blocking can be explained, as mentioned above, by the absorption of part of the ultraviolet light by beeswax (Huang, Huang, Xu, & Liu, 2022).

3.2. Chemical characterization

CGW bioplastics were chemically characterized by ATR-FTIR spectroscopy, Fig. 2A. Fig. S1 displays the ATR-FTIR of pure cellulose, glycerol, and beeswax. CGW-0 showed the typical bands previously described for glycerol-plasticized cellulose films (Benitez et al., 2024): O-H stretching mode at ~3320 cm^{-1}, asymmetric and symmetric CH_2 stretching modes at ~2920 and ~2880 cm^{-1}, respectively, a band associated with adsorbed water at ~1650 cm^{-1}, CH_2 deformation mode at ~1455 cm^{-1}, bands associated with the ring vibration of the anhydroglucose unit of cellulose at ~1155 and ~900 cm^{-1}, and CH_2 rocking mode at ~925 cm^{-1}. No bands associated with the solvent mixture were detected, confirming the complete evaporation during the drying process (Guzman-Puyol et al., 2015). CGW-5 and CGW-20 films showed some additional bands ascribed to beeswax such as the asymmetric and

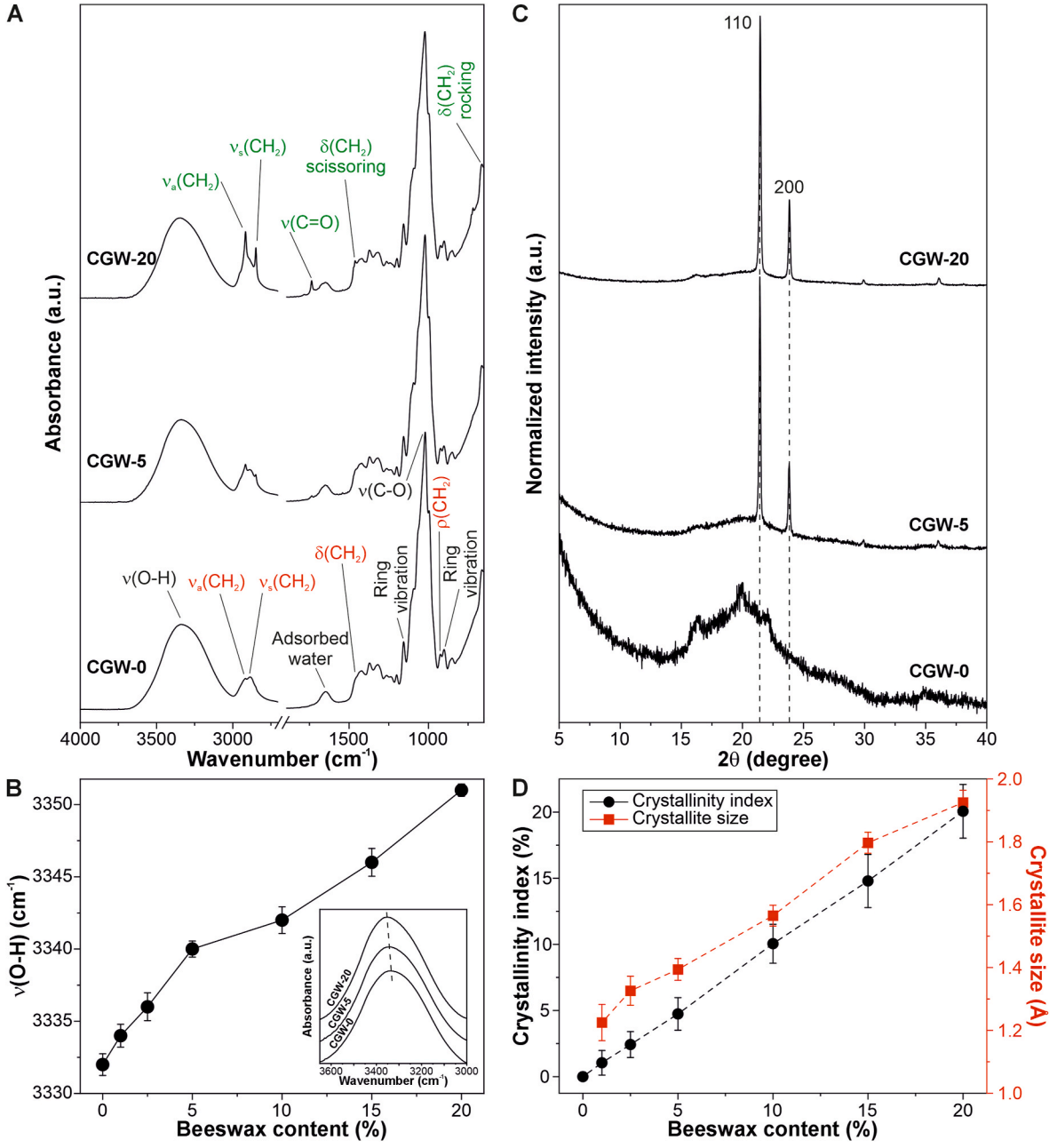

Fig. 2. A, ATR-FTIR spectra of CGW-0, CGW-5, and CGW-20. The assignment of the main bands is included for cellulose (black), glycerol (red), and beeswax (green). **B,** shift of the O-H stretching mode with the beeswax content. Inset: O-H stretching band of CGW-0, CGW-5, and CGW-20. **C,** X-ray diffractograms of CGW-0, CGW-5, and CGW-20. **D,** crystallinity index and crystallite size as a function of beeswax content.

symmetric CH_2 stretching modes at 2915 and 2847 cm^{-1}, respectively, the stretching mode of C=O at ~1735 cm^{-1}, CH_2 scissoring mode at ~1460 cm^{-1}, and CH_2 rocking mode at ~720 cm^{-1}. Interestingly, a shift associated with the O-H stretching mode with the beeswax content was observed, Fig. 2B. The wavenumber of this band increased from ~3332 cm^{-1} for CGW-0 to ~3351 cm^{-1} for CGW-20 (i.e., a difference of 19 cm^{-1}). Such an increase in the wavenumber can be attributed to weaker and longer H-bonds due to the intercalation of beeswax crystals within the polymer matrix, that effectively separate cellulose polymer chains, thus hindering the interaction between the OH groups of cellulose and glycerol.

The crystallinity of CGW bioplastics was determined by XRD, Fig. 2C. CGW-0 displayed a diffractogram typical of amorphous cellulose materials, with a broad halo at ~20°, as previously described in literature (Bayer et al., 2014; Guzman-Puyol, Tedeschi, et al., 2022). For CGW-5 and CGW-20, some peaks were observed at ~21 and ~24°, ascribed to the crystalline planes (110) and (200) of beeswax, respectively (Naderizadeh et al., 2019). From XRD diffractograms, the crystallinity index and crystallite size were calculated, Fig. 2D. For the crystallinity, a linear increase (with a slope close to 1.0) was observed by increasing the beeswax content, with values of ~1 % for CGW-1, ~5 % for CGW-5, and ~20 % for CGW-20. This is indicative of an almost complete crystallization of all beeswax (mainly in plates randomly distributed, as observed by SEM). On the other hand, the crystallite size was also increased with the beeswax percentage due to the aggregation of a higher amount of beeswax molecules.

3.3. Mechanical characterization

Mechanical properties of CGW bioplastics were analyzed by stress-strain curves, Fig. 3A. For CGW-0, typical values of glycerol-plasticized cellulose bioplastics prepared by solution in TFA:TFAA were obtained, with Young's modulus of ~963 MPa, ultimate tensile strength of ~31 MPa, and strain at break of ~20% (Benitez et al., 2024). Addition of beeswax affected significantly the mechanical properties of CGW bioplastics, reducing progressively all main mechanical parameters (i.e., Young's modulus, ultimate tensile strength, strain at break, and toughness), Fig. 3B. This behavior has been previously described for

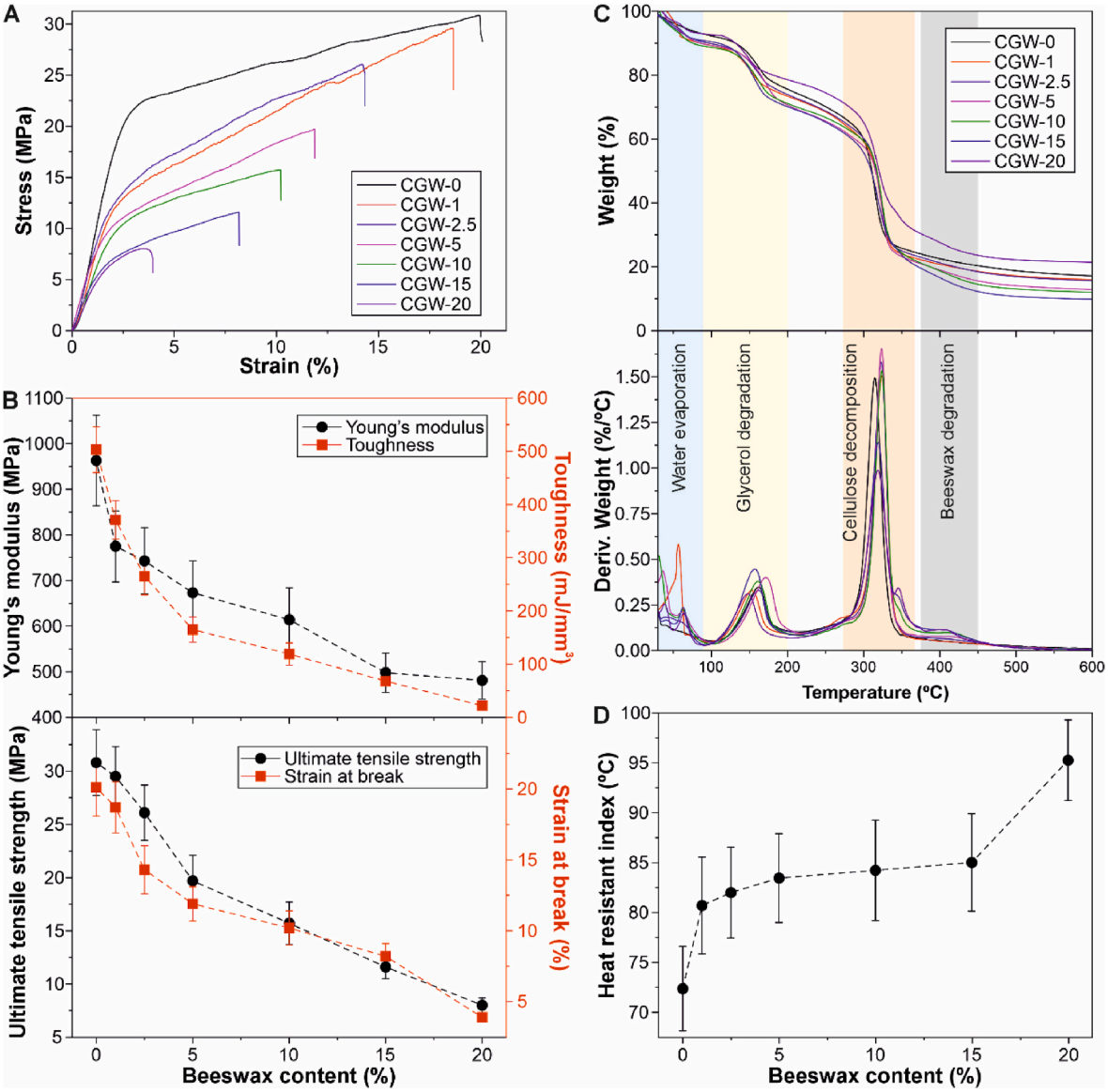

Fig. 3. A, typical stress-strain curves of CGW samples. **B,** Young's modulus, toughness, ultimate tensile strength, and strain at break values as a function of beeswax content. **C,** TGA thermograms (top) and the corresponding derivative curves (bottom) of CGW bioplastics. **D,** heat resistant index of CGW samples as a function of beeswax content.

other beeswax-containing polysaccharide-based and protein-based materials (Fabra, Talens, Gavara, & Chiralt, 2012; Hromiš et al., 2015). For Young's modulus, initial values were ~963 MPa for CGW-0 and ~673 MPa for CGW-5, similar to high density polyethylene (HDPE) and PP, whereas for CGW-20 the value was reduced by half (~481 MPa), being this value similar to the one of commercial LDPE bags (Benitez et al., 2024; Guzman-Puyol, Hierrezuelo, et al., 2022). Toughness values also decreased by the addition of beeswax, with values of ~503 mJ/mm^3 for CGW-0, ~165 mJ/mm^3 for CGW-5, and ~22 mJ/mm^3 for CGW-20. Regarding the ultimate tensile strength (UTS), values ranged from ~31 MPa for CGW-0 to ~20 MPa for CGW-5 and ~8 MPa for CGW-20. These values were similar to the values of common LDPE (12 MPa), HDPE (30 MPa), and PP (35 MPa). Finally, elongation at break values were also reduced by increasing the beeswax content with values of ~20% for CGW-0, ~12% for CGW-5, and ~4% for CGW-20. These values were found close to other common food packaging materials such as PLA, PVC, and polystyrene (PS) (19, 15, and 3%, respectively) (Benitez et al., 2024). As observed, incorporating beeswax into the cellulose:glycerol blend results in a reduction of all mechanical parameters. Typically, for blends, the rearrangement of the H-bond network caused by the proportions of the components induces mechanical changes where a parameter is increased and other decreased, e.g., the tensile strength and the elongation at break (Priyadarshi, Kim, & Rhim, 2021). However, for the cellulose:glycerol:beeswax blends, their weakening of mechanical properties can be attributed to the disruption of the hydrogen-bond network within the material matrix, as evidenced by the reduction in the O-H stretching mode in FTIR analysis described above. The presence of beeswax, a non-polar material, interrupts the cohesive hydrogen bonds between the cellulose chains and glycerol molecules by physically intercalating within the matrix. This intercalation hinders the formation of hydrogen bonds between the hydroxyl groups of cellulose and glycerol, which are essential for mechanical robustness.

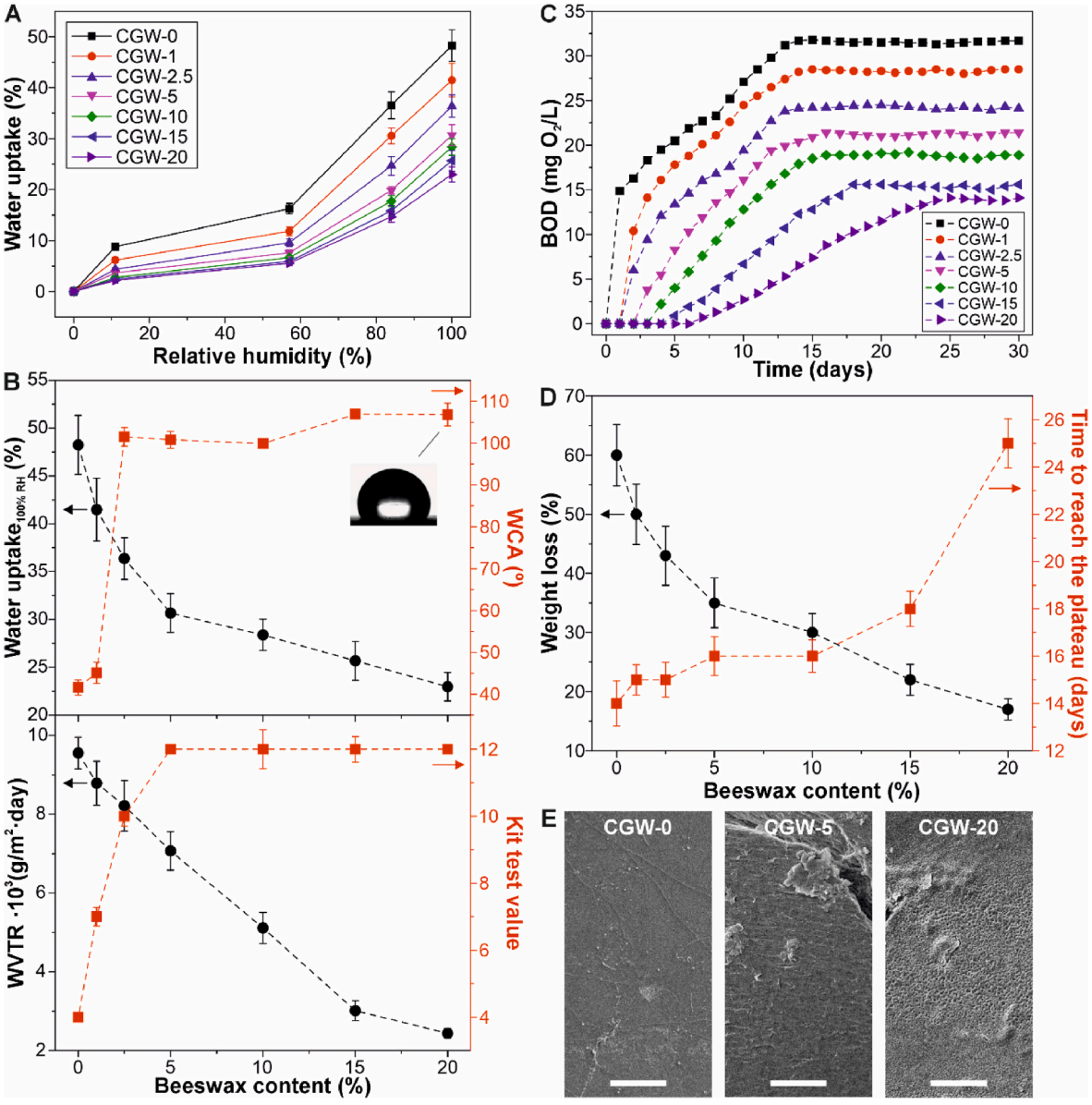

Fig. 4. **A,** water uptake of CGW bioplastics as a function of the relative humidity. **B**, top, variation of water uptake at 100% RH and water contact angle and, bottom, water vapor transmission rates and kit test values of CGW bioplastics with the beeswax content. The inset shows a water drop on CGW-20. **C,** representative biological oxygen demand (BOD) curves as a function of time for each CGW films. **D,** weight losses after 30 days of BOD tests and time to reach the plateau of CGW bioplastics as a function of beeswax content. **E,** top-view SEM images of CGW-0, CGW-5, and CGW-20 after BOD tests. Scale bar: 50 μm.

3.4. Thermal characterization

The thermal stability of CGW bioplastics was assessed by TGA, Fig. 3C. TGA curves and their corresponding derivative curves showed four main peaks. The first one at ~59 °C was ascribed to the evaporation of adsorbed water. A second weight loss between 148 and 173 °C was related to the decomposition of glycerol into water, formaldehyde, and acetaldehyde (Zhang et al., 2021). A decrease in the temperature of decomposition of glycerol by increasing the beeswax content was observed, with values ranging from ~173 °C for CGW-0, ~162 °C for CGW-5, and ~148 °C for CGW-20, most probably due to the weaker interaction between glycerol molecules when beeswax was present. An almost constant third thermal event was found at ~320 °C and was associated with cellulose decomposition. Finally, a weight loss at ~345 °C was attributed to the thermal decomposition of beeswax, as expected by comparison with the TGA of pure beeswax, Fig. S2.

From TGA curves, the heat resistant index was calculated as an estimation of the maximum temperature at which CGW bioplastics can be used without significant degradation (Hafiezal, Khalina, Zurina, Azaman, & Hanafee, 2019), Fig. 3D and S3. Pure beeswax presented a heat resistant index of 149 °C. For CGW-0, heat resistant index was ~72.4 °C, increasing to an almost constant value of ~85 °C for beeswax percentages between 1 and 10 wt.-%. For CGW-20, a higher heat resistant index of ~95.3 °C was observed. As showed, the inclusion of beeswax had a positive effect on the thermal properties of CGW bioplastics, expanding the range of temperatures in which these materials can be used.

3.5. Hydrodynamic, water barrier, and greaseproof characterization

Water isotherms of CGW bioplastics were determined by the quantification of the water uptake at different relative humidities, Fig. 4A. All CGW samples showed adsorption isotherms type II according to IUPAC classification, typical of nonporous materials (Eddaoudi, 2005) and previously described for other cellulose-based materials (Guzman-Puyol et al., 2015), being the values lower by increasing the beeswax content. Fig. 4B shows the water uptake values at 100% RH, the water contact angle, the water barrier properties, and greaseproof performance of CGW samples as a function of beeswax content. As expected, a decay was observed in the water uptake at 100% RH, with values of ~48.3% for CGW-0, ~30.7% for CGW-5, and ~23.0% for CGW-20, Fig. 4B (top). As displayed, the inclusion of 20% beeswax reduced by half the water uptake values. However, all these values were still high, being similar to other food packaging materials such as polyvinyl alcohol (PVA) and polysaccharide-based materials such as pullulan and chitosan films (~20 and ~30%, respectively) (Guzman-Puyol et al., 2015; Kristo & Biliaderis, 2007; Remuñán-López & Bodmeier, 1997).

The wettability of CGW bioplastics was investigated by determination of the water contact angle, Fig. 4B (top). For CGW-0, a low value of ~42° was obtained, typical of hydrophilic cellulose substrates. Addition of 1 wt% beeswax slightly increased the water contact angle to a value of ~45°. For the rest of the samples, an almost constant water contact value of ~105° was obtained. Such a hydrophobicity can be explained both by the non-polar chemical components of beeswax and the roughness of the beeswax plates on the CGW films' surfaces observed by SEM, indicating that beeswax tends to crystallize on the cellulose-glycerol film. These values are similar of those of some fluorinated polymers such as ethylene-chlorotrifluoroethylene copolymer or ECTFE (99°) and ethylene-tetrafluoroethylene copolymer or ETFE (108°) (Lee, Park, & Randall Lee, 2008) and some other common petroleum-based materials currently used in food packaging applications such as LDPE (95°), PS (95°), and PP (111°) (Extrand, 2003; Kwon, Tang, Myung, Lu, & Choi, 2005; Meiron & Saguy, 2007) and are consistent with the increment of water contact angles of other polysaccharide-based films when waxes were added (Indriyati, Frecilla, Nuryadin, Irmawati, & Srikandace, 2020).

Water barrier properties of CGW films were also evaluated through determination of the water vapor transmission rate and permeability, Fig. 4B (bottom) and S4. In general, water permeability was almost linearly reduced by increasing the percentage of crystalline beeswax, from values of ~9500 g/m^{2}day for CGW-0, to ~7000 g/m^{2}day for CGW-5, about a 26% of reduction, and ~2400 g/m^{2}day for CGW-20, a decrease of ~75% with respect to the initial value, being similar to other food packaging materials such as cellulose acetate (2120 g/m^{2}day), vegetable and wrap papers (2324 and 2588 g/m^{2}day, respectively), and chitosan films (2682 g/m^{2}day) (Guzman-Puyol, Hierrezuelo, et al., 2022; Guzman-Puyol, Tedeschi, et al., 2022). Such a decrease can be related to the intrinsic impermeability of beeswax crystals, that act as effective barriers against water (Wu et al., 2021).

The greaseproof behavior of CGW bioplastics was tested by the kit test. For CGW-0, a kit test value of ~4 was measured, corresponding to a low barrier level against oil according to the limit of kit test higher than 5 stablished by the TAPPI standard (Sheng, Li, & Zhao, 2019). Kit test values were highly affected by the addition of beeswax, with values of ~7 for CGW-1 and ~10 for CGW-2.5. For beeswax contents above 5 wt %, the obtained value was ~12, the highest kit test value, demonstrating the feasibility of these CGW films to resist the direct contact with fats and oils.

3.6. Biodegradation in seawater

The biodegradability of CGW samples was assessed through the determination of the biological oxygen demand in seawater for 30 days, Fig. 4C. A progressive delay of the start of degradation was observed by increasing the beeswax content, with values, for example, of 1, 3, and 7 days for CGW-0, CGW-5, and CGW-20, respectively. It is also remarkable the inverse correlation between final biodegradation values and beeswax contents. Thus, for CGW-0 the final BOD value was ~31.7 mg O_2/L, decreasing to a value of ~21.4 mg O_2/L for CGW-5 and ~14.1 mg O_2/L for CGW-20. The time to reach the plateau and the weight loss after the BOD tests were also measured for the different samples, Fig. 4D. Interestingly, the time to reach the plateau showed a similar behavior to the delay in the degradation process. On the other hand, for the weight loss, a decay by increasing the beeswax content was observed. In general, all these decrease of biodegradation parameters can be related to the crystallinity and non-polar character of beeswax, as confirmed by XRD and WCA measurements, that hinder the interaction with water and, hence, with the marine bacterial population that produce the biodegradation. However, even for beeswax-rich bioplastics, these values are characteristic of biodegradable polymers such as cellulose acetate and ethyl cellulose (5 and 11%, respectively) and much higher than those of common polymers such as polyethylene terephthalate (PET), PLA, and LDPE (0 %) (Guzman-Puyol, Tedeschi, et al., 2022). After BOD, CGW films pieces were recovered and SEM was used to characterize the main differences in their morphology, Fig. 4E. CGW-0 surface showed the typical eroded and heterogeneous previously reported for cellulose-based materials (Guzman-Puyol, Hierrezuelo, et al., 2022; Guzman-Puyol, Tedeschi, et al., 2022). For CGW-5 and CGW-20, more eroded surfaces were observed, with some protuberances and holes homogeneously distributed, most probably due to the physical removing of the beeswax crystalline plates during the BOD tests.

3.7. Assessment of CGW bioplastics as active food packaging materials

3.7.1. Antioxidant capacity, overall migration, and preservation of pear slices

The antioxidant capacity of CGW films was assessed by using the DPPH radical scavenging protocol, Fig. 5A. A gradually increase of the antioxidant capacity for higher beeswax contents was observed. Thus, CGW-0 showed the lowest antioxidant capacity with final radical scavenging activity (RSA) values of ~3.3% after 96 h, as previously reported for other cellulose-based materials (Guzman-Puyol, Hierrezuelo, et al.,

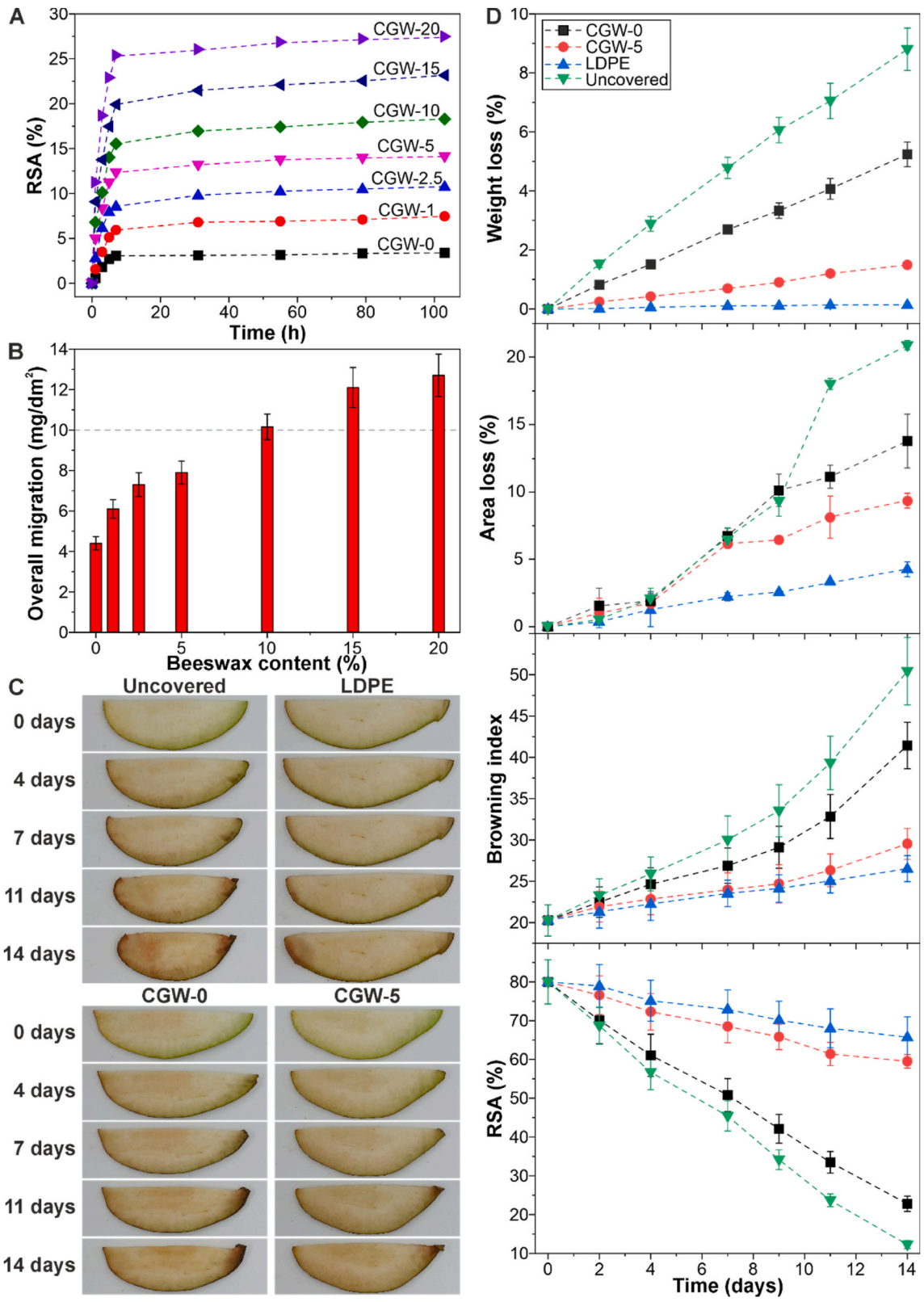

Fig. 5. A, antioxidant capacity of CGW samples calculated by using the DPPH· method. **B,** overall migration of CGW bioplastics to Tenax® dry food simulant. **C,** photographs of pear slices uncovered and covered with LDPE, CGW-0, and CGW-5 films after 0, 4, 7, 11, and 14 days. **D**, weight loss, browning index, and antioxidant capacity of pear slices as a function of the storage time.

2022), followed by CGW-1 (~7.5%), CGW-2.5 (~10.8%), CGW-5 (~14.1%), CGW-10 (~18.3%), CGW-15 (~23.2%), and CGW-20 with the highest antioxidant capacity (~27.5%). This increase in the antioxidant activity of CGW bioplastics can be explained by the presence of antioxidant polyphenols such as kaempferol, apigenin, and pinobanksin naturally present in beeswax (Martinello & Mutinelli, 2021; Sawicki, Starowicz, Kłębukowska, & Hanus, 2022).

The overall migration of CGW bioplastics was tested by using Tenax® as a dry food simulant, Fig. 5B. For CGW-0, the overall migration was (4.4 ± 0.3) mg/dm^2, increasing progressively until values of (6.1 ± 0.5) mg/dm^2 for CGW-1, (7.3 ± 0.6) mg/dm^2 for CGW-2.5, and (7.9 ± 0.6) mg/dm^2 for CGW-5, below the threshold stated by the European Commission Regulation October 2011 about plastics intended to be in contact with food (10 mg/dm^2) (Commission, 2011). On the other hand, for the beeswax-richer samples, overall migration values were (10.2 ± 0.6), (12.1 ± 1), and (12.7 ± 1.1) mg/dm^2 for CGW-10, CGW-15, and CGW-20, respectively, thus being not suitable for food packaging applications.

As a proof of concept, CGW-0 and CGW-5 bioplastics, both below EU migration limits, were selected to further check their viability as food packaging of fresh-cut pear slices, Fig. 5C and D. For the control (uncovered pear slices), a drastic shrinkage and browning was observed during the storage time, Fig. 5C. On the contrary, in the same period, for the pears covered with LDPE films, pear slices did not almost change in size and color. For the pear slices covered with CGW-0 and CGW-5, both size reduction and browning were less pronounced than uncovered pears. To further characterize the preservation of pear slices, their weight and area losses, browning index, and antioxidant capacity were measured at different storage times, Fig. 5D. For the weight loss, a rapid linear increase was observed for the uncovered pear slices, with final values of ~8.8% after 14 days, while for those covered with LDPE, an almost constant weight loss was measured, with very low values of ~0.1% after 14 days. For pears covered with CGW-0 and CGW-5, an intermediate behavior was observed, with final weight loss values of ~5.2 and ~1.5%, respectively. These results are in agreement with the visual changes previously described and can be explained by the improved water vapor barrier properties of LDPE and CGW-5, that prevent the massive water loss during storage. Area loss measurements were conducted to quantify the reduction in size, which is only slightly noticeable by visual inspection. As observed, all samples exhibited similar behavior up to day 4. Starting from day 4, the LDPE sample, from day 7, CGW-5, and from day 9, CGW-0, showed area losses lower than the uncovered sample. Similar to weight loss, after 14 days, the LDPE covering resulted in the lowest area loss (~4.3%), while the uncovered sample showed the highest area loss (~20.9%). The CGW-0 and CGW-5 coverings displayed intermediate values of ~13.8% and ~9.4%, respectively. These changes can be attributed to the ability of the different films to prevent significant water loss, as described above. Browning index was chosen as a more accurate indicator of the color changes of pear slices over time, usually ascribed to different enzymatic and non-enzymatic reactions naturally occurring in fresh fruits and vegetables (Hosseini, Mousavi, & McClements, 2023). For the uncovered pear slices and those covered with CGW-0, an exponential increase of the browning index was measured, especially after 9 days in the fridge. For these samples, browning index after 14 days were ~50.4 for uncovered pears and ~41.4 for pears covered with CGW-0 films. For CGW-5 and LDPE, a linear increase was measured, with very close final values (~29.5 and ~26.5, respectively). The differences found among CGW samples can be explained by the enhanced antioxidant activity of CGW-5 due to the presence of beeswax, that can effectively neutralize free radicals from pear slices and the higher oxygen barrier properties of CGW-5, that reduce the oxygen permeation into the package, reducing the product oxidation. Finally, the antioxidant capacity of the fruit at the different storage times was checked by using the DPPH radical scavenging method. In general, a linear decrease was observed, being the decay faster for the uncovered pears, followed by the ones covered with CGW-0. The antioxidant capacity of pears covered with CGW-5 were found to be slightly lower than those of pears covered with LDPE and are consistent with the values of browning index previously described and the oxygen permeability values, Fig. 6B, indicating the contribution of beeswax to actively protect food and extend the shelf-life.

3.7.2. Antimicrobial capacity and oxygen barrier properties

The antimicrobial activity of selected CGW-0 and CGW-5 bioplastics was tested by using different bacteria (*Escherichia coli* and *Bacillus cereus*), Fig. 6A. *E. coli* and *B. cereus* are foodborne pathogens that can cause significant health issues when ingested through contaminated food or water. *E. coli* is a broad family of coliform bacteria that can lead to severe gastrointestinal distress, including bloody diarrhea and kidney failure. These pathogens are often linked to undercooked ground beef, raw vegetables, and unpasteurized dairy products (Niveditha et al., 2021). On the other hand, *B. cereus* is a spore-forming bacterium typical of starchy foods that may produce toxins causing diarrhea and vomiting (Jovanovic, Ornelis, Madder, & Rajkovic, 2021). As showed, no inhibition halo was observed, insets of Fig. 6A, most probably due to the no migration of beeswax molecules from films to polar culture media. On the other hand, retentivity tests were also carried out to assess the capability of CGW bioplastics to hold fixed bacteria, thus reducing the possibilities of eventual bacterial propagation to food. As showed, CGW-0 and CGW-5 presented higher retentivity capacity than LDPE films used as a control. In particular, for CGW-5 bioplastics, retentivity values were improved ~25% when *E. coli* was used and ~18% for *B. cereus* with respect to the control. Such a higher retentivity capacity is also linked with the low retentivity values measured for the agar, demonstrating the capacity of CGW samples to actively protect food from pathogenic bacteria.

Finally, the oxygen barrier properties of CGW-0 and CGW-5 bioplastics were characterized at different relative humidities, Fig. 6B. In general, the oxygen permeabilities of CGW-0 and CGW-5 were affected by relative humidity, showing a gradual increase of oxygen permeability values by increasing the relative humidity as previously reported for other polymers such as ethylene vinyl alcohol (EVOH), cellophane, and methyl cellulose (Gontard, Thibault, Cuq, & Guilbert, 1996). At 0% RH, CGW-0 and CGW-5 showed oxygen permeability values of ~$0.006{\cdot}10^{-18}$ and ~$0.004{\cdot}10^{-18}$ kg m m^{-2} s^{-1} Pa^{-1}, respectively, being these values lower than those described for cellophane (Wang et al., 2018) or polyamide (Robertson, 2016). At the highest relative humidity, oxygen permeability values were ~$8.719{\cdot}10^{-18}$ and ~$18.931{\cdot}10^{-18}$ kg m m^{-2} s^{-1} Pa^{-1}, for CGW-0 and CGW-5, respectively, similar to oriented polypropylene (OPP), a common packaging material for fresh and fresh-cut fruits and vegetables. Furthermore, Fig. 6C reports a comparison of oxygen permeability values at 60% RH. of CGW-0 and CGW-5 with other common food packaging plastics and bioplastics. CGW-0 and CGW-5 showed higher oxygen permeability values than EVOH (*Kurakay*, 2024) and similar to those of PET and PLA (Fernández-Menéndez, García-López, Argüelles, Fernández, & Viña, 2020; Robertson, 2016). Other common food packaging materials such as OPP, LDPE, and protein-based bioplastics showed higher oxygen permeability values than CGW-0 and CGW-5 (Pranata et al., 2019; Robertson, 2016).

4. Conclusions

In this work, active food packaging materials have been fabricated by addition of beeswax to glycerol-plasticized cellulose matrices. Chemical and structural characterization showed a modification of the H-bond network and an increase of the crystallinity. As a result, transparency and mechanical properties were negatively affected, but still with values similar to common petroleum-based food packaging plastics. The addition of beeswax improved the hydrodynamic properties, with an important decrease of water uptake and water vapor transmission rate values. Moreover, CGW bioplastics showed high resistance to oils and

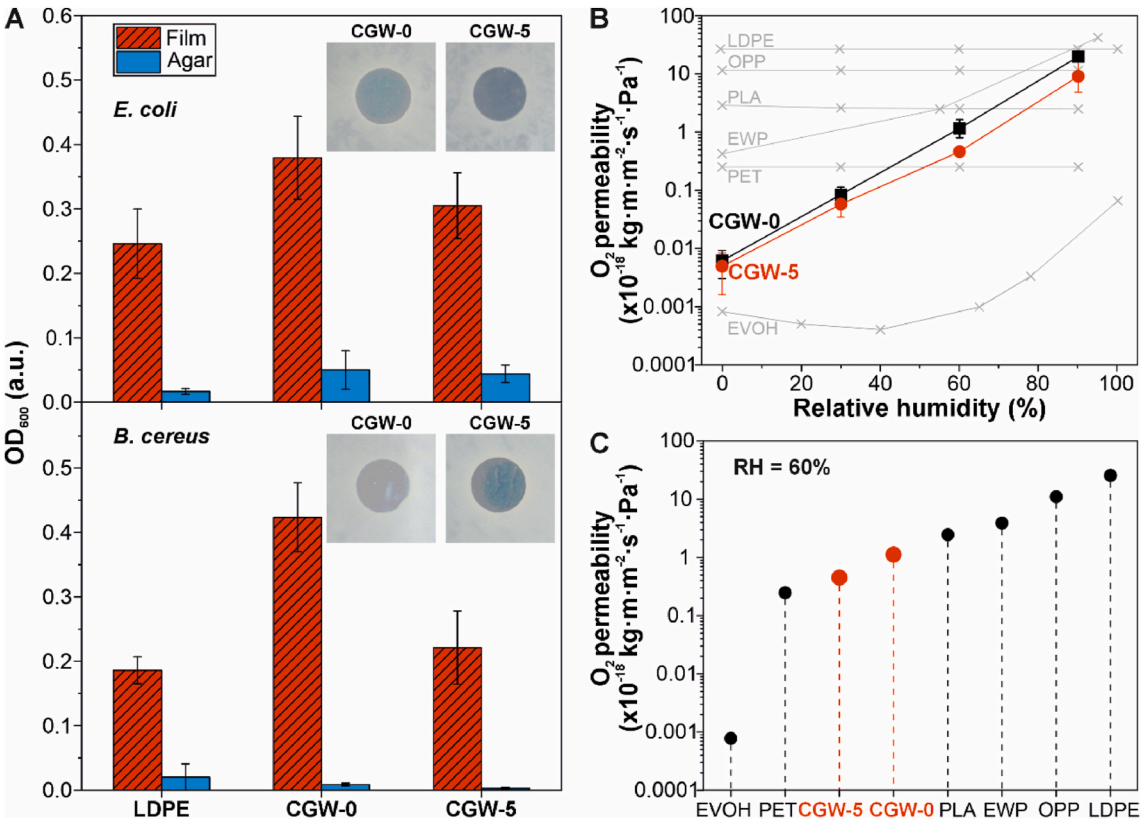

Fig. 6. A, bacterial retentivity tests of *E. coli* and *B. cereus* on CGW-0 and CGW-5 bioplastics. The insets show photographs of the inhibition halo tests. **B,** oxygen permeability of CGW-0 and CGW-5 as a function of relative humidity. Grey symbols and lines represent data of from literature for common plastics and bioplastics. **C,** comparison of oxygen permeability values at 60% RH of CGW samples with other common materials used in food packaging.

fats, antioxidant capacity, and biodegradability in seawater.

To further check the convenience of CGW bioplastics as food packaging materials, overall migrations were determined, resulting in good performances for beeswax content up to 5 wt.- %. Fresh-cut pear slices preserved with CGW-5 presented similar appearance, weight and area losses, browning index, and antioxidant capacity to those preserved with commercial LDPE films. Regarding the antibacterial properties, these films showed a high bacterial retention capacity, thus potentially avoiding the propagation of pathogens towards the food. Finally, oxygen permeability measured at medium range relative humidities (60%), showed a similar behavior to high barrier food packaging materials such as PLA and PET and better than LDPE.

This study addresses the urgent need for sustainable packaging alternatives in the food industry. By enhancing cellulose:glycerol films with beeswax, we improve barrier properties and stability, essential for maintaining product quality. These findings lay the groundwork for scalable, eco-friendly bioplastics, aligning with industry trends toward sustainable packaging solutions.

CRediT authorship contribution statement

Pedro Florido-Moreno: Writing – review & editing, Investigation. **José J. Benítez:** Writing – review & editing, Investigation. **Jaime González-Buesa:** Writing – review & editing, Investigation. **José M. Porras-Vázquez:** Writing – review & editing, Investigation. **Jesús Hierrezuelo:** Writing – review & editing, Investigation. **Montserrat Grifé-Ruiz:** Writing – review & editing, Investigation. **Diego Romero:** Writing – review & editing, Investigation. **Athanassia Athanassiou:** Writing – review & editing, Investigation. **José A. Heredia-Guerrero:** Writing – review & editing, Writing – original draft, Investigation, Funding acquisition, Conceptualization. **Susana Guzmán-Puyol:** Writing – review & editing, Writing – original draft, Supervision, Investigation, Funding acquisition, Conceptualization.

Declaration of competing interest

None.

Acknowledgements

This work has been partially supported by the Spanish Research Council (CSIC) project 202040E003. S.G-P thanks the "Consejería de Transformación Económica, Industria, Conocimiento y Universidades" from Junta de Andalucía for her postdoctoral contract (POST-DOC_21_00008). The authors thank Cristina Amella for her assistance in preparing samples for the OTR tests and María del Rocío Muñoz-Pérez for her assistance in the preservation assay of pear slices.

Appendix A. Supplementary data

Supplementary data to this article can be found online at https://doi.org/10.1016/j.foodhyd.2024.110933.

Data availability

Data will be made available on request.

References

Alee, M., Duan, Q., Chen, Y., Liu, H., Ali, A., Zhu, J., et al. (2021). Plasticization efficiency and characteristics of monosaccharides, disaccharides, and low-molecular-weight polysaccharides for starch-based materials. *ACS Sustainable Chemistry & Engineering, 9*(35). https://doi.org/10.1021/acssuschemeng.1c04374

Almeida, M. M. B., de Sousa, P. H. M., Arriaga, Á. M. C., do Prado, G. M., Magalhães, C. E. de C., Maia, G. A., et al. (2011). Bioactive compounds and

antioxidant activity of fresh exotic fruits from northeastern Brazil. *Food Research International, 44*(7). https://doi.org/10.1016/j.foodres.2011.03.051
Andreuccetti, C., Carvalho, R. A., & Grosso, C. R. F. (2009). Effect of hydrophobic plasticizers on functional properties of gelatin-based films. *Food Research International, 42*(8). https://doi.org/10.1016/j.foodres.2009.05.010
Aubry, C., & Kebir, L. (2013). Shortening food supply chains: A means for maintaining agriculture close to urban areas? The case of the French metropolitan area of Paris. *Food Policy, 41*. https://doi.org/10.1016/j.foodpol.2013.04.006
Baghi, F., Gharsallaoui, A., Dumas, E., & Ghnimi, S. (2022). Advancements in biodegradable active films for food packaging: Effects of nano/microcapsule incorporation. In *Foods* (Vol. 11). https://doi.org/10.3390/foods11050760. Issue 5.
Bayer, I. S., Guzman-Puyol, S., Heredia-Guerrero, J. A., Ceseracciu, L., Pignatelli, F., Ruffilli, R., et al. (2014). Direct transformation of edible vegetable waste into bioplastics. *Macromolecules, 47*(15), 5135–5143. https://doi.org/10.1021/ma5008557
Benitez, J. J., Florido-Moreno, P., Porras-Vázquez, J. M., Tedeschi, G., Athanassiou, A., Heredia-Guerrero, J. A., et al. (2024). Transparent, plasticized cellulose-glycerol bioplastics for food packaging applications. *International Journal of Biological Macromolecules, 273*, Article 132956. https://doi.org/10.1016/J.IJBIOMAC.2024.132956
Caligiuri, V., Tedeschi, G., Palei, M., Miscuglio, M., Martin-Garcia, B., Guzman-Puyol, S., et al. (2020). Biodegradable and insoluble cellulose photonic crystals and metasurfaces. *ACS Nano, 14*(8), 9502–9511. https://doi.org/10.1021/acsnano.0c03224
Cazón, P., Velazquez, G., Ramírez, J. A., & Vázquez, M. (2017). Polysaccharide-based films and coatings for food packaging: A review. *Food Hydrocolloids, 68*. https://doi.org/10.1016/j.foodhyd.2016.09.009
Commission, E.. (2011). Commission Regulation (EU) No 10/2011 of 14 January 2011 on plastic materials and articles intended to come into contact with food. *Official Journal of the European Union, 12*, 1–89.
Cornara, L., Biagi, M., Xiao, J., & Burlando, B. (2017). Therapeutic properties of bioactive compounds from different honeybee products. In *Frontiers in pharmacology* (Vol. 8). https://doi.org/10.3389/fphar.2017.00412. Issue JUN.
Dong, Y., Li, Y., Ma, Z., Rao, Z., Zheng, X., Tang, K., et al. (2023). Effect of polyol plasticizers on properties and microstructure of soluble soybean polysaccharide edible films. *Food Packaging and Shelf Life, 35*. https://doi.org/10.1016/j.fpsl.2022.101023
Eddaoudi, M. (2005). Characterization of Porous Solids and Powders: Surface Area, Pore Size and Density By S. Lowell (Quantachrome Instruments, Boynton Beach), J. E. Shields (C. W. Post Campus of Long Island University), M. A. Thomas, and M. Thommes (Quantachrome In-struments). Kluwer Academic Publishers: Dordrecht, The Netherlands. 2004. xiv + 348 pp. $159.00. ISBN 1-4020-2302-2. *Journal of the American Chemical Society, 127*(40). https://doi.org/10.1021/ja041016i
EFSA. (2007). Beeswax (E 901) as a glazing agent and as carrier for flavours - Scientific Opinion of the Panel on Food additives, Flavourings, Processing aids and Materials in Contact with Food (AFC). *EFSA Journal, 5*(12). https://doi.org/10.2903/j.efsa.2007.615
Extrand, C. W. (2003). Contact angles and hysteresis on surfaces with chemically heterogeneous islands. *Langmuir, 19*(9). https://doi.org/10.1021/la0268350
Ezati, P., Khan, A., Priyadarshi, R., Bhattacharya, T., Tammina, S. K., & Rhim, J. W. (2023). Biopolymer-based UV protection functional films for food packaging. In *Food hydrocolloids* (Vol. 142). https://doi.org/10.1016/j.foodhyd.2023.108771
Fabra, M. J., Talens, P., Gavara, R., & Chiralt, A. (2012). Barrier properties of sodium caseinate films as affected by lipid composition and moisture content. *Journal of Food Engineering, 109*(3). https://doi.org/10.1016/j.jfoodeng.2011.11.019
Fernández-Menéndez, T., García-López, D., Argüelles, A., Fernández, A., & Viña, J. (2020). Industrially produced PET nanocomposites with enhaced properties for food packaging applications. *Polymer Testing, 90*. https://doi.org/10.1016/j.polymertesting.2020.106729
Geyer, R., Jambeck, J. R., & Law, K. L. (2017). Production, use, and fate of all plastics ever made. *Science Advances, 3*(7). https://doi.org/10.1126/sciadv.1700782
Gontard, N., Thibault, R., Cuq, B., & Guilbert, S. (1996). Influence of relative humidity and film composition on oxygen and carbon dioxide permeabilities of edible films. *Journal of Agricultural and Food Chemistry, 44*(4). https://doi.org/10.1021/jf9504327
Guzman-Puyol, S. (2024). Fluorinated compounds in paper and paperboard based food packaging materials. *Npj Science of Food, 8*(1), 1–7. https://doi.org/10.1038/s41538-024-00326-2, 2024 8:1.
Guzman-Puyol, S., Benítez, J. J., & Heredia-Guerrero, J. A. (2022). Transparency of polymeric food packaging materials. *Food Research International, 161*, Article 111792. https://doi.org/10.1016/J.FOODRES.2022.111792
Guzman-Puyol, S., Ceseracciu, L., Heredia-Guerrero, J. A., Anyfantis, G. C., Cingolani, R., Athanassiou, A., et al. (2015). Effect of trifluoroacetic acid on the properties of polyvinyl alcohol and polyvinyl alcohol–cellulose composites. *Chemical Engineering Journal, 277*, 242–251. https://doi.org/10.1016/J.CEJ.2015.04.092
Guzman-Puyol, S., Hierrezuelo, J., Benítez, J. J., Tedeschi, G., Porras-Vázquez, J. M., Heredia, A., et al. (2022). Transparent, UV-blocking, and high barrier cellulose-based bioplastics with naringin as active food packaging materials. *International Journal of Biological Macromolecules, 209*, 1985–1994. https://doi.org/10.1016/j.ijbiomac.2022.04.177
Guzman-Puyol, S., Tedeschi, G., Goldoni, L., Benítez, J. J., Ceseracciu, L., Koschella, A., et al. (2022). Greaseproof, hydrophobic, and biodegradable food packaging bioplastics from C6-fluorinated cellulose esters. *Food Hydrocolloids, 128*, Article 107562. https://doi.org/10.1016/J.FOODHYD.2022.107562
Hafiezal, M. R. M., Khalina, A., Zurina, Z. A., Azaman, M. D. M., & Hanafee, Z. M. (2019). Thermal and flammability characteristics of blended jatropha bio-epoxy as matrix in carbon fiber–reinforced polymer. *Journal of Composites Science, 3*(1). https://doi.org/10.3390/jcs3010006
Heredia-Guerrero, J. A., Benítez, J. J., Porras-Vázquez, J. M., Tedeschi, G., Morales, Y., Fernández-Ortuño, D., et al. (2023). Plasticized, greaseproof chitin bioplastics with high transparency and biodegradability. *Food Hydrocolloids, 109072*. https://doi.org/10.1016/J.FOODHYD.2023.109072
Hosseini, S. F., Mousavi, Z., & McClements, D. J. (2023). Beeswax: A review on the recent progress in the development of superhydrophobic films/coatings and their applications in fruits preservation. In *Food chemistry* (Vol. 424). https://doi.org/10.1016/j.foodchem.2023.136404
Hromiš, N. M., Lazić, V. L., Markov, S. L., Vaštag, Ž. G., Popović, S. Z., Šuput, D. Z., et al. (2015). Optimization of chitosan biofilm properties by addition of caraway essential oil and beeswax. *Journal of Food Engineering, 158*. https://doi.org/10.1016/j.jfoodeng.2015.01.001
Huang, H., Huang, C., Xu, C., & Liu, R. (2022). Development and characterization of lotus-leaf-inspired bionic antibacterial adhesion film through beeswax. *Food Packaging and Shelf Life, 33*. https://doi.org/10.1016/j.fpsl.2022.100906
Indriyati, Frecilla, N., Nuryadin, B. W., Irmawati, Y., & Srikandace, Y. (2020). Enhanced Hydrophobicity and Elasticity of Bacterial Cellulose Films by Addition of Beeswax. *Macromolecular Symposia, 391*(1). https://doi.org/10.1002/masy.201900174
Jovanovic, J., Ornelis, V. F. M., Madder, A., & Rajkovic, A. (2021). Bacillus cereus food intoxication and toxicoinfection. *Comprehensive Reviews in Food Science and Food Safety, 20*(4). https://doi.org/10.1111/1541-4337.12785
Kristo, E., & Biliaderis, C. G. (2007). Physical properties of starch nanocrystal-reinforced pullulan films. *Carbohydrate Polymers, 68*(1). https://doi.org/10.1016/j.carbpol.2006.07.021
Kurakay. (2024) https://eval.kuraray.com/products-services/about-eval-evoh/properties/barrier-to-oxygen.
Kwon, O. J., Tang, S., Myung, S. W., Lu, N., & Choi, H. S. (2005). Surface characteristics of polypropylene film treated by an atmospheric pressure plasma. *Surface and Coatings Technology, 192*(1). https://doi.org/10.1016/j.surfcoat.2004.09.018
Lee, S., Park, J.-S., & Randall Lee, T. (2008). The Wettability of Fluoropolymer Surfaces: Influence of Surface Dipoles. *Langmuir, 24*(9), 4817–4826. https://doi.org/10.1021/la700902h
Lim, J. H., Kim, J. A., Ko, J. A., & Park, H. J. (2015). Preparation and Characterization of Composites Based on Polylactic Acid and Beeswax with Improved Water Vapor Barrier Properties. *Journal of Food Science, 80*(11). https://doi.org/10.1111/1750-3841.13081
Liu, R., Zhang, R., Zhai, X., Li, C., Hou, H., & Wang, W. (2022). Effects of beeswax emulsified by octenyl succinate starch on the structure and physicochemical properties of acid-modified starchfilms. *International Journal of Biological Macromolecules, 219*. https://doi.org/10.1016/j.ijbiomac.2022.07.235
Marsh, K., & Bugusu, B. (2007). Food packaging - Roles, materials, and environmental issues: Scientific status summary. In *Journal of food science* (Vol. 72, pp. R39–R55). John Wiley & Sons, Ltd. https://doi.org/10.1111/j.1750-3841.2007.00301.x. Issue 3.
Martinello, M., & Mutinelli, F. (2021). Antioxidant activity in bee products: A review. In *Antioxidants* (Vol. 10). https://doi.org/10.3390/antiox10010071. Issue 1.
Meiron, T. S., & Saguy, I. S. (2007). Wetting properties of food packaging. *Food Research International, 40*(5). https://doi.org/10.1016/j.foodres.2006.11.010
Morillon, V., Debeaufort, F., Blond, G., Capelle, M., & Voilley, A. (2002). Factors affecting the moisture permeability of lipid-based edible films: A review. *Critical Reviews in Food Science and Nutrition, 42*(1). https://doi.org/10.1080/10408690290825466
Naderizadeh, S., Heredia-Guerrero, J. A., Caputo, G., Grasselli, S., Malchiodi, A., Athanassiou, A., et al. (2019). Superhydrophobic Coatings from Beeswax-in-Water Emulsions with Latent Heat Storage Capability. *Advanced Materials Interfaces, 6*(5). https://doi.org/10.1002/admi.201801782
Niveditha, A., Pandiselvam, R., Prasath, V. A., Singh, S. K., Gul, K., & Kothakota, A. (2021). Application of cold plasma and ozone technology for decontamination of Escherichia coli in foods- a review. In *Food control* (Vol. 130). https://doi.org/10.1016/j.foodcont.2021.108338
Pascale, R., Acquavia, M. A., Onzo, A., Cataldi, T. R. I., Calvano, C. D., & Bianco, G. (2023). Analysis of surfactants by mass spectrometry: Coming to grips with their diversity. In *Mass spectrometry reviews* (Vol. 42). https://doi.org/10.1002/mas.21735. Issue 5.
Peron, G., Carmo dos Santos, N. A., Ferrarese, I., Rizzo, F., Bernabè, G., Paccagnella, M., et al. (2023). The beeswax processing by-product: a potential antibacterial ingredient for food and nutraceutical applications. *International Journal of Food Science and Technology, 58*(10). https://doi.org/10.1111/ijfs.16520
Pranata, M. P., González-Buesa, J., Chopra, S., Kim, K., Pietri, Y., Ng, P. K. W., et al. (2019). Egg White Protein Film Production Through Extrusion and Calendering Processes and its Suitability for Food Packaging Applications. *Food and Bioprocess Technology, 12*(4), 714–727. https://doi.org/10.1007/S11947-019-2248-0, 2019 12: 4.
Priyadarshi, R., Kim, S. M., & Rhim, J. W. (2021). Pectin/pullulan blend films for food packaging: Effect of blending ratio. *Food Chemistry, 347*. https://doi.org/10.1016/j.foodchem.2021.129022
Remuñán-López, C., & Bodmeier, R. (1997). Mechanical, water uptake and permeability properties of crosslinked chitosan glutamate and alginate films. *Journal of Controlled Release, 44*(2–3). https://doi.org/10.1016/S0168-3659(96)01525-8
Robertson, G. L. (2016). Food Packaging: Principles and Practice. In *Food packaging: Principles and practice* (3rd ed.). Third Edition. https://doi.org/10.1201/b21347.
Sawicki, T., Starowicz, M., Kłębukowska, L., & Hanus, P. (2022). The Profile of Polyphenolic Compounds, Contents of Total Phenolics and Flavonoids, and

Antioxidant and Antimicrobial Properties of Bee Products. *Molecules, 27*(4). https://doi.org/10.3390/molecules27041301

Sheng, J., Li, J., & Zhao, L. (2019). Fabrication of grease resistant paper with non-fluorinated chemicals for food packaging. *Cellulose, 26*(10), 6291–6302. https://doi.org/10.1007/s10570-019-02504-y

Siracusa, V., Rocculi, P., Romani, S., & Rosa, M. D. (2008). Biodegradable polymers for food packaging: a review. In *Trends in food science and technology* (Vol. 19). https://doi.org/10.1016/j.tifs.2008.07.003. Issue 12.

Smith, P. (2015). Malthus is still wrong: We can feed a world of 9-10 billion, but only by reducing food demand. In *Proceedings of the nutrition society* (Vol. 74). https://doi.org/10.1017/S0029665114001517, 3.

Tedeschi, G., Guzman-Puyol, S., Ceseracciu, L., Benitez, J. J., Goldoni, L., Koschella, A., et al. (2021). Waterproof-breathable films from multi-branched fluorinated cellulose esters. *Carbohydrate Polymers, 271*, Article 118031. https://doi.org/10.1016/J.CARBPOL.2021.118031

Trinh, B. M., Chang, B. P., & Mekonnen, T. H. (2023). The barrier properties of sustainable multiphase and multicomponent packaging materials: A review. In *Progress in materials science* (Vol. 133). https://doi.org/10.1016/j.pmatsci.2023.101071

Vieira, M. G. A., da Silva, M. A., dos Santos, L. O., & Beppu, M. M. (2011). Natural-based plasticizers and biopolymer films: A review. *European Polymer Journal, 47*(3), 254–263. https://doi.org/10.1016/j.eurpolymj.2010.12.011

Wang, J., Gardner, D. J., Stark, N. M., Bousfield, D. W., Tajvidi, M., & Cai, Z. (2018). Moisture and Oxygen Barrier Properties of Cellulose Nanomaterial-Based Films. *ACS Sustainable Chemistry & Engineering, 6*(1), 49–70. https://doi.org/10.1021/acssuschemeng.7b03523

Wu, F., Misra, M., & Mohanty, A. K. (2021). Challenges and new opportunities on barrier performance of biodegradable polymers for sustainable packaging. In *Progress in polymer science* (Vol. 117). https://doi.org/10.1016/j.progpolymsci.2021.101395

Zhang, D., Cao, Y., Zhang, P., Liang, J., Xue, K., Xia, Y., et al. (2021). Investigation of the thermal decomposition mechanism of glycerol: the combination of a theoretical study based on the Minnesota functional and experimental support. *Physical Chemistry Chemical Physics, 23*(36), 20466–20477. https://doi.org/10.1039/D1CP01526E